

See discussions, stats, and author profiles for this publication at: <https://www.researchgate.net/publication/7885266>

# Hybrid Nanocapsules : Interactions of ABA Block Copolymers with Liposomes

ARTICLE *in* JOURNAL OF THE AMERICAN CHEMICAL SOCIETY · JUNE 2005

Impact Factor: 12.11 · DOI: 10.1021/ja043600x · Source: PubMed

---

CITATIONS

74

---

READS

23

6 AUTHORS, INCLUDING:



[Mathias Winterhalter](#)

Jacobs University

213 PUBLICATIONS 5,559 CITATIONS

SEE PROFILE

## Hybrid Nanocapsules: Interactions of ABA Block Copolymers with Liposomes

Tristan Ruyschaert,<sup>†</sup> Andreas F. P. Sonnen,<sup>‡,§</sup> Thomas Haeefe,<sup>#</sup> Wolfgang Meier,<sup>#</sup> Mathias Winterhalter,<sup>†,‡</sup> and Didier Fournier<sup>\*,†</sup>

*Groupe de Biotechnologie des Protéines, Institut de Pharmacologie et de Biologie Structurale, 31077, Toulouse, France, International University Bremen, D-28726 Bremen, Germany, Department of Physical Chemistry, University of Basel, Klingelbergstrasse 80, CH-4056, Basel, Switzerland*

Received October 21, 2004; Revised Manuscript Received March 8, 2005; E-mail: didier.fournier@ipbs.fr

**Abstract:** Amphiphilic ABA triblock copolymers, such as poly(2-methyloxazoline)-block-poly(dimethylsiloxan)-block-poly(2-methyloxazoline) (PMOXA-PDMS-PMOXA), form vesicular structures. Here, the interaction of these ABA molecules with lipids is investigated by electron microscopy, fluorescence spectroscopy, light scattering, and differential scanning calorimetry. Our observations suggest the formation of homogeneous mixed polymer–lipid composites, independent of preparation method, i.e. film hydration, dispersion, or detergent removal. When ABA polymersomes and liposomes are mixed, we observed monomer exchanges on a time scale of minutes. The possibility of forming mixed structures and the exchanges between preformed structures allow the combination of the properties of lipids and polymers such as stability and loading encapsulation capacity.

### Introduction

Self-assembly of amphiphilic phospholipids may result in the formation of vesicular aggregates constituted by a lipid bilayer that is stabilized by hydrophobic interactions. Classical liposomes, as described by Bangham et al.,<sup>1</sup> have an aqueous core domain surrounded by a hydrophobic lipid bilayer, thus mimicking cells or subcellular compartments that are sealed by biological membranes. As model systems, they are extensively employed to investigate in vitro protein reconstitution, organelle fusion, endo and exocytosis, viral infection, and membrane permeation induced by toxins or channel-forming proteins.<sup>2,3</sup> For example, as vehicles for drug delivery, liposomes are able to transport water-soluble cargo in their core domain and lipophilic antioxidants inside the hydrophobic parts of the bilayer to prevent lipid peroxidation. However, unmodified liposomes suffer from a low stability against shear forces, extreme pH's, and osmotic stress. In vivo, rapid enzymatic degradation is followed by opsonization, which triggers uptake by the mononuclear phagocytic system.<sup>4</sup> Hence exploiting the self-assembly properties of lipids for technical applications requires stabiliza-

tion of the formed structures. Several approaches based on cross-linking the lipid itself have been summarized by Ringsdorf et al.<sup>5</sup>

Biological membranes are adapted to the cell machinery and find applications in many other areas. Recently attempts have been made to replace lipids by self-assembling amphiphilic block copolymers, to tailor size, form, and stability specifically for individual applications.<sup>6</sup> Notably, AB, ABA, and ABC block copolymers were shown to form micelles, vesicles, or "sponge"-like aggregates.<sup>6</sup> AB diblock copolymers preferentially form micelles, driven by segregation of the core from the aqueous milieu, due to a combination of intermolecular forces including hydrophobic, electrostatic, and hydrogen-bonding interactions.<sup>7,8</sup> A prominent, medically most relevant example are micelles based on adriamycin cross-linked poly(ethylene glycol)-poly( $\alpha,\beta$ -aspartic acid) diblock copolymers, which possess antitumor activity.<sup>9</sup>

ABA block copolymers such as the poly(ortho ester)-poly(ethylene glycol)-poly(ortho ester) triblock copolymer formed microspheres with encapsulated protein.<sup>10</sup> Vesicular structures could be formed in water when solubilizing ABA triblock copolymers, composed of a hydrophobic and flexible poly(dimethylsiloxane) (PDMS) middle block and two water-soluble

<sup>†</sup> Institut de Pharmacologie et de Biologie Structurale.

<sup>‡</sup> International University Bremen.

<sup>§</sup> Current address: Department of Biochemistry and The Division of Structural Biology, University of Oxford, U.K.

<sup>#</sup> University of Basel.

(1) Bangham, A. D.; Standish, M. M.; Watkins, J. C. *J. Mol. Biol.* **1965**, *13*, 238–52.

(2) Masin, J.; Konopasek, I.; Svobodova, J.; Sebo, P. *Biochim. Biophys. Acta* **2004**, *1660*, 144–54.

(3) Takeuchi, K.; Takahashi, H.; Sugai, M.; Iwai, H.; Kohno, T.; Sekimizu, K.; Natori, S.; Shimada, I. *J. Biol. Chem.* **2004**, *279*, 4981–7.

(4) Papahadjopoulos, D.; Allen, T. M.; Gabizon, A.; Mayhew, E.; Matthey, K.; Huang, S. K.; Lee, K. D.; Woodle, M. C.; Lasic, D. D.; Redemann, C. *Proc. Natl. Acad. Sci. U.S.A.* **1991**, *88*, 11460–4.

(5) Ringsdorf, H.; Schlarb, B.; Venzmer, J. *Angew. Chem., Int. Ed. Engl.* **1988**, *27*, 113–158.

(6) Discher, D. E.; Eisenberg, A. *Science* **2002**, *297*, 967–73.

(7) Dan, N.; Safran, S. A. *Macromolecules* **1994**, *27*, 5766–72.

(8) Kataoka, K.; Harada, A.; Nagasaki, Y. *Adv. Drug Deliv. Rev.* **2001**, *47*, 113–31.

(9) Yokoyama, M.; Miyauchi, M.; Yamada, N.; Okano, T.; Sakurai, Y.; Kataoka, K.; Inoue, S. *Cancer Res.* **1990**, *50*, 1693–700.

(10) Yang, Y. Y.; Wan, J. P.; Chung, T. S.; Pallathadka, P. K.; Ng, S.; Heller, J. J. *Control Release* **2001**, *75*, 115–28.

poly(2-methyloxazoline) (PMOXA) side blocks.<sup>10–13</sup> In a somewhat surprising result it was shown that despite the 2–3-fold higher thickness of the block copolymer membranes, proteins could be readily integrated and remained functional even after polymerization of reactive block copolymer end-groups.<sup>14</sup> These chimera assemblies allow the preparation of mechanically stable, defect-free nanocapsules with a highly selective permeability.<sup>15</sup> At least two features of the polymer membrane facilitated protein miscibility: (i) polymer chains can be compressed considerably due to the high flexibility of the PDMS block and (ii) polydispersity of the polymer allows small chains to segregate around a membrane protein.<sup>14</sup>

The aim of this work is to study the mixing behavior of amphiphilic triblock copolymers with lipids and the feasibility of forming mixed lipid–polymer nanoparticles. We added lipid and ABA during the vesicle formation and obtained mixed structures. Transmission electron microscopy (TEM), dynamic light scattering (DLS), differential scanning calorimetry (DSC), and fluorescence experiments suggested that lipids were homogeneously distributed in these binary composites. We also observed molecular exchange between liposomes and ABA nanocapsules by fluorescence resonance energy transfer (FRET).

## Experimental Section

**Materials.** The lipids, egg-phosphatidylethanolamine (PE), brain L $\alpha$ -PS (PS), L $\alpha$ -phosphatidylethanolamine-*N*-(lissamine-rhodamine-B-sulfonyl) (Rhod-PE), L $\alpha$ -phosphatidylethanolamine-*N*-(4-nitrobenzo-2-oxa-1,3-diazole) (NBD-PE), and dipalmitoylphosphatidylcholine (DPPC) were purchased from Avanti Polar Lipids (Birmingham, AL). Egg-phosphatidylcholine (PC) was from Lipoid (Ludwigshafen, Germany). Calcein high purity was obtained from Molecular Probes (Leiden, The Netherlands). PMOXA-PDMS-PMOXA triblock copolymer, with a molecular weight of 9000 g mol<sup>-1</sup>, i.e., a PDMS middle block of 5400 g mol<sup>-1</sup> and of two hydrophilic PMOXA blocks each of 1800 g mol<sup>-1</sup>, was synthesized as described earlier.<sup>12</sup> The polydispersity was determined to be  $M_w/M_n = 1.7$ .

**Formation of Vesicles.** Three methods were used to obtain lipids, ABA block copolymers, and mixed vesicles. In the ethanol injection method, 200  $\mu$ L of clear ethanol solution of 17 wt % PMOXA-PDMS-PMOXA triblock copolymer was added dropwise to 5 mL of vigorously stirred buffer D (145 mM NaCl, 2.5 mM HEPES, pH 7.4).<sup>16</sup> This technique led to vesicles of 50 nm average diameter. In the film hydration technique, lipids were dissolved in chloroform and dried at the bottom of a glass tube under nitrogen and then for 3 h under vacuum to remove all remaining traces of solvent.<sup>17</sup> The film was solubilized by addition of buffer D and vortexing for 1 min. Finally, 10 freeze–thaw cycles followed by extrusion through a 200 nm polycarbonate cut-off membrane, using a Hamilton syringe extruder (Avanti Polar Lipids, Birmingham, AL), gave monolamellar vesicles. The same procedure was followed for ABA and the ABA–lipid mixture except that the solubilization time was extended to 30 min and the extrusion step was eliminated. The diameter was 200 nm for lipid and 500 nm for ABA vesicles; that of the mixed aggregates varied between these two values. In the detergent removal method, a homogeneous film of ABA or/and lipids was made as described above for the film hydration

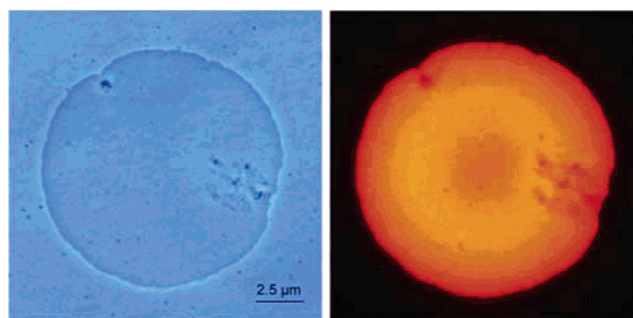


**Figure 1.** Giant particle composed of a mixture of ABA and lipids observed by phase contrast and fluorescence microscopy using rhodamine-labeled phosphatidylethanolamine.

method, but solubilization was enhanced by addition of 1% (vol/vol) Triton X-100 (TX-100) to buffer D. Following solubilization, the detergent was completely removed by addition of 150 mg/mL Bio-Beads (SM-2 Absorbent, Bio-Rad Laboratories, 20–50 mesh) and overnight incubation under continuous rotational stirring.<sup>18</sup> Vesicles with a diameter from 50 to 150 nm were obtained, depending on the ABA/lipid composition.

Giant ABA/lipid vesicles were prepared as previously described.<sup>19</sup> Briefly, 500  $\mu$ L containing 5 mg of ABA/PC/PE/Rhod-PE (79/12/8/1, mol/mol/mol) dissolved in chloroform was sprayed on two indium tin oxide coated glass electrodes (Merck LCD division). Chloroform was removed under nitrogen and vacuum. Electrodes were immersed in buffer D using a Teflon spacer. Vesicles were formed by applying a simple ac voltage of 5 V at a frequency of 10 Hz for 3 h and 5 V at 0.5 Hz for 30 min. Vesicles were observed under a fluorescence microscope with a 100 $\times$  Zeiss plan apochromat objective.

**Enzyme Encapsulation.** A film of lipid and/or ABA (1  $\mu$ mol) was solubilized with 200  $\mu$ L of buffer D, containing 4 nmol of *Drosophila melanogaster* acetylcholinesterase (AChE). Twenty-five freeze thaw cycles were performed to allow for protein encapsulation.<sup>20,21</sup> Nonencapsulated AChE was removed by inverse affinity chromatography, i.e. by passing the polymersome suspension through a procainamide gel column that retains free AChE. Buffer D was added to reach a concentration of 1 mM lipid/ABA. Amounts of encapsulated protein were estimated by measuring the AChE activity with the Ellman method<sup>22</sup> after total disruption of the polymersomes with 0.1% TX-100. Solubilization of the ABA/lipid mixed polymersomes by this detergent was verified by light scattering.<sup>23</sup>

**Fluorescence.** Rhod-PE ( $\lambda_{ex} = 550$  nm/ $\lambda_{em} = 590$  nm), NBD-PE ( $\lambda_{ex} = 470$  nm/ $\lambda_{em} = 530$  nm), and calcein ( $\lambda_{ex} = 492$  nm/ $\lambda_{em} = 517$  nm) were used as fluorescent probes. The distribution of lipids was estimated via the self-quenching of Rhod-PE. Different concentrations of fluorescently labeled lipids were incorporated into egg-PC/egg-PE (2/1, mol/mol) liposomes, in which Rhod-PE homogeneously distributes. ABA vesicles were also labeled with Rhod-PE. Fluorescence was measured in intact vesicles (IF) and after destruction (IF0) with 1% TX-100, causing almost infinite dilution of the probe accompanied by disappearance of self-quenching.

Fluorescence resonance energy transfer (FRET) was determined using NBD as energy donor, and rhodamine as energy acceptor.<sup>24</sup>

- (11) Nardin, C.; Winterhalter, M.; Meier, W. *Langmuir* **2000**, *16*, 7708–12.
- (12) Nardin, C.; Hirt, T.; Leukel, J.; Meier, W. *Langmuir* **2000**, *16*, 1035–41.
- (13) Graff, A.; Sauer, M.; Van Gelder, P.; Meier, W. *Proc. Natl. Acad. Sci. U.S.A.* **2002**, *99*, 5064–8.
- (14) Nardin, C.; Meier, W. *Rev. Mol. Biotechnol.* **2002**, *90*, 17–26.
- (15) Meier, W.; Nardin, C.; Winterhalter, M. *Angew. Chem., Int. Ed.* **2000**, *39*, 4599–4602.
- (16) Kremer, J. M.; Esker, M. W.; Pathmanathan, C.; Wiersema, P. H. *Biochemistry* **1977**, *16*, 3932–5.
- (17) Lichtenberg, D.; Barenholz, Y. *Methods Biochem. Anal.* **1988**, *33*, 337–462.

- (18) Ueno, M.; Tanford, C.; Reynolds, J. A. *Biochemistry* **1984**, *23*, 3070–6.
- (19) Sauer, M.; Haelele, T.; Graff, A.; Nardin, C.; Meier, W. *Chem. Commun. (Cambridge)* **2001**, 2452–3.
- (20) Chaize, B.; Winterhalter, M.; Fournier, D. *Biotechniques* **2003**, *34*, 1158–60, 1162.
- (21) Colletier, J. P.; Chaize, B.; Winterhalter, M.; Fournier, D. *BMC Biotechnol.* **2002**, *2*, 9.
- (22) Ellman, G. L.; Courtney, K. D.; Andres, V., Jr.; Feather-Stone, R. M. *Biochem. Pharmacol.* **1961**, *7*, 88–95.
- (23) Pata, V.; Ahmed, A.; Discher, D. E.; Dan, N. *Langmuir* **2004**, *20*, 3888–93.
- (24) Struck, D. K.; Hoekstra, D.; Pagano, R. E. *Biochemistry* **1981**, *20*, 4093–9.

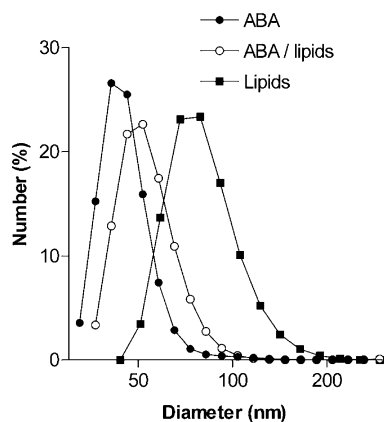


**Figure 2.** DLS analysis of particles obtained by the detergent removal method with ABA, lipids, and a mixture of ABA and lipids.

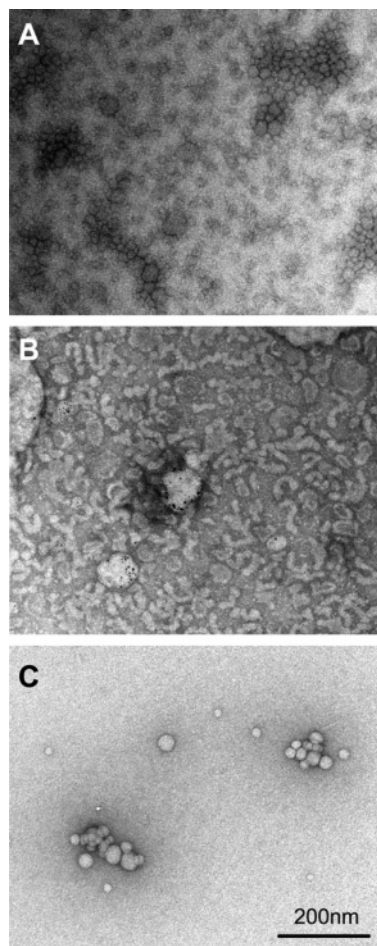


**Figure 3.** TEM of ABA (A), PC/PE liposomes (B), and ABA/PC/PE mixed vesicles (C) formed by the detergent removal technique.

Liposomes were labeled with 0.6 mol % of NBD-PE and Rhod-PE, respectively. FRET efficiency was determined by the ratio of the NBD fluorescence (470/530 nm) before (IF) and after TX-100 addition (0.5% final) (IF0) corrected for sample dilution and the effect of TX-100 on the quantum yield of N-NBD-PE (multiplication by a factor of 1.4 in our experimental conditions). FRET efficiency is thus related to (IF/IF0) and increases during membrane dilution corresponding to a FRET efficiency decrease.

To follow ABA-induced membrane perturbation, liposomes containing concentrated calcein were prepared. Calcein (3 mM) was encapsulated

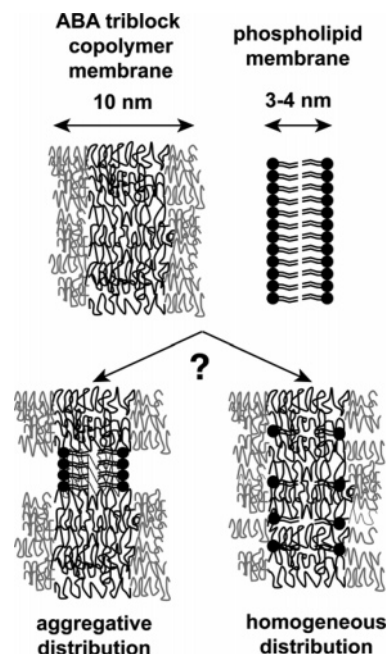


**Figure 4.** Hypothetic structures of hybrid membranes composed of ABA triblock copolymers and lipids. Lipids might either segregate into domains leading to an aggregative distribution or disperse in an ABA triblock membrane in a homogeneous phase.

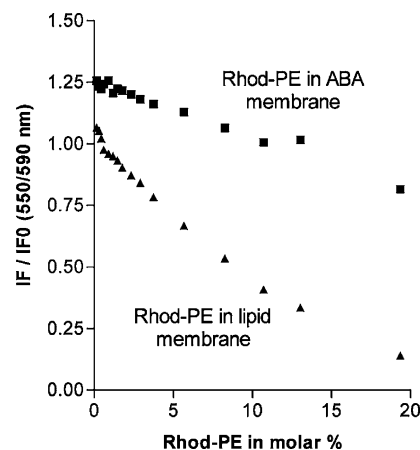


**Figure 5.** Self-quenching of Rhod-PE in an egg-PC/egg-PE (2/1) lipid membrane (▲) and in an ABA membrane (■). Self-quenching of Rhod-PE was quantified by the ratio of IF/IF0, where IF is the fluorescence of the labeled lipid in the absence of TX100 and IF0 is the fluorescence after solubilizing the membrane caused by addition of 0.5% TX-100. Concentrations of ABA + Rhod-PE or lipid + Rhod-PE were 0.05 mM.

solated into liposomes by 20 freeze–thaw cycles.<sup>25</sup> Free calcein was removed by  $6 \times 10^6$  dilution in buffer D using dialysis through a 10 kDa cutoff membrane. After ABA addition fluorescence increase (IF) due to calcein efflux was determined. Total release (IF0) was estimated by liposome destruction using 0.5% TX-100.

**Transmission Electron Microscopy (TEM) and Dynamic Light Scattering (DLS).** Nanoparticles were negatively stained with 2% uranyl acetate solution, deposited on a carbon-coated copper grid, and examined with a Philips Morgagni 268D microscope. Size distribution of particles was estimated using a Zetasizer Nano ZS90 (Malvern Instruments, Malvern, UK) with 90° optics and a He–Ne Laser (4.0 mW, 633 nm).

**Differential Scanning Calorimetry (DSC).** DSC measurements of the ABA-DPPC hybrid nanocapsules and lipid-only liposomes were

(25) MacDonald, R. I. *J. Biol. Chem.* **1990**, *265*, 13533–9.



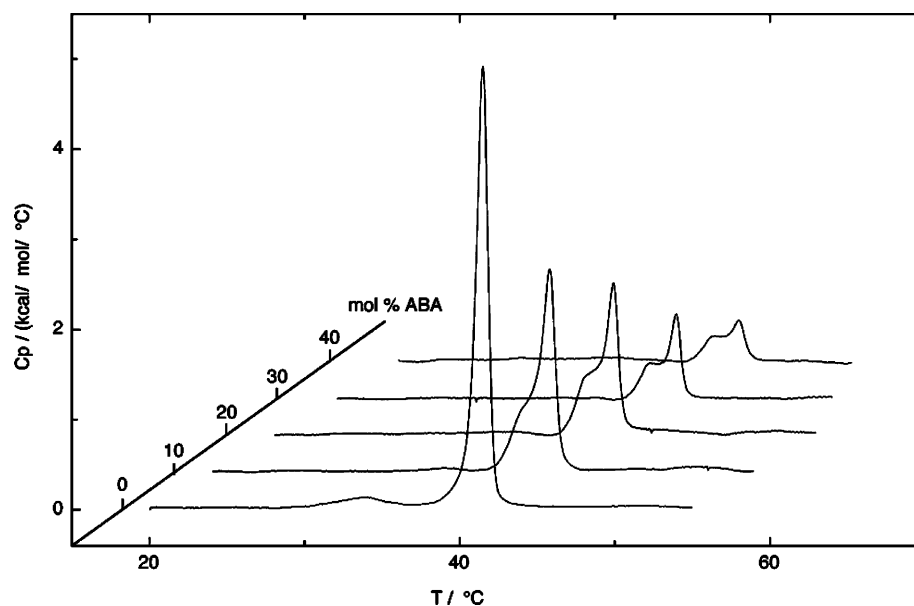


**Figure 6.** DSC experiments showing the endotherms of DPPC (1 mg/mL) with increasing ABA content.

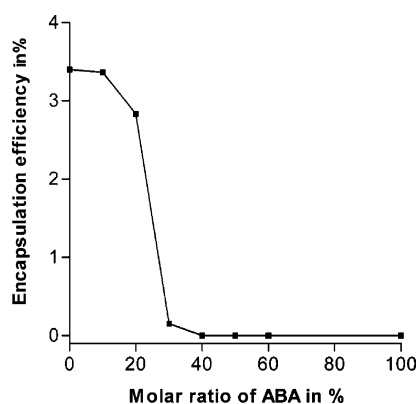


**Figure 7.** AChE encapsulation efficiency of hybrid ABA/lipid particles after 25 freeze–thaw cycles. Encapsulation efficiency is given in % of the final versus the total initial enzymatic activity, and the total concentration of ABA and lipid was together 1 mM. The final enzymatic activity was revealed by Pronase digestion of the nonencapsulated enzyme and revealing the encapsulated activity by vesicle disruption with 0.1% TX-100 (see Experimental Section for details).

performed with a VP-DSC (Microcal Inc., Northampton, MA). A temperature range of 10–70 °C was scanned with a heating rate of 30 K/h and a filter period of 1. Data were analyzed with Origin 5.0 (OriginLab Co., Northampton, MA).

## Results and Discussion

### Evidence for Mixing of ABA and Lipid in Giant Particles.

Giant ABA vesicles with fluorescently labeled lipids were prepared to investigate the mixing behavior of ABA and lipids. If mixed structures of ABA and lipid are formed, all particles should be fluorescent due to an incorporation of lipids. By contrast, in the absence of mixing, a binary system composed of fluorescent liposomes and nonfluorescently labeled ABA particles should be obtained. Only large fluorescent aggregates with a non perfectly spherical shape could be observed (Figure 1). Neither giant nonfluorescent ABA particles nor a structure resembling giant liposomes<sup>26</sup> was observed by using a mixture

of lipid and ABA. Hence, we conclude that ABA and lipids may form mixed particles.

**Evidence for Mixed ABA/Lipid Nanoparticles.** ABA and lipid vesicles, prepared by the detergent removal method, were analyzed by DLS and TEM. ABA and PC lipid alone yielded particles with an average diameter of 53 and 112 nm, respectively (Figure 2). When vesicles were prepared using a mixture of ABA and PC (3/1, mol/mol), we observed a monomodal size distribution of particles with an average diameter of 75 nm. This suggests the formation of hybrid particles. TEM of ABA alone gave spherical particles around 50 nm in diameter (Figure 3A). Liposomes alone (PC/PE; 2/1 mol/mol) did not resist dehydration, leading to collapsed structures (Figure 3B). An ABA lipid mixture (ABA/PC/PE, 7/2/1 mol/mol/mol) did not result in the formation of two distinct populations of particles, and spheres similar to those obtained for ABA alone could be observed. Hence DLS and TEM analysis are consistent, in that hybrid particles are formed when using a mixture of ABA and lipids. Hybrid particles seem to be as stable as ABA polymersomes, not collapsing upon dehydration.

**ABA/Lipid Distribution in Mixed Vesicles.** Both lipid and ABA might form separate domains, leading to a heterogeneous membrane structure, or might distribute homogeneously in the same phase, as illustrated in Figure 4. For a low lipid to ABA ratio we choose a fluorescence quenching technique with Rhod-PE, which allowed us to compare the self-quenching of Rhod-PE in lipid membrane to the self-quenching in ABA membrane. We measured the fluorescence emitted from the particles before (IF) and after solubilization with detergent (IF0). For Rhod-PE incorporated into liposomes a decrease of IF/IF0 with increasing probe concentration was observed (Figure 5). This is a typical feature of increased self-quenching as reported for similar systems by Mac Donald.<sup>25</sup> As it can be assumed that Rhod-PE is homogeneously distributed in the lipid bilayer, the curve in Figure 5 is indicative for quenching in the nonaggregative state. Similarly, a decrease of IF/IF0 with increasing Rhod-PE concentration, with a slope similar to that observed in the pure lipid system, was also obtained for the mixed particles. These results suggest a nonaggregative distribution of lipids in ABA

(26) Angelova, M. I.; Dimitrov, S. A. *Faraday Discuss. Chem. Soc.* **1986**, *81*, 303–11.

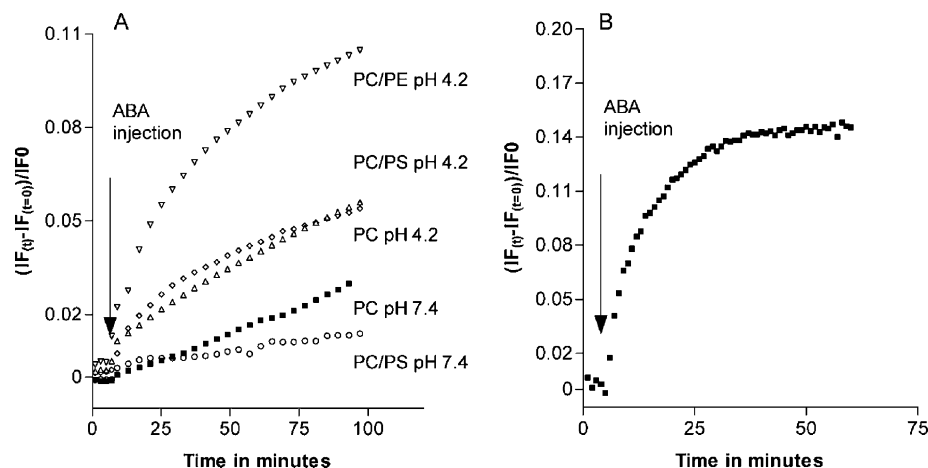


**Figure 8.** Addition of ABA vesicles to liposome induces lipid dilution and transient pore formation. (A) Increase of NBD-PE fluorescence due to dilution of lipids in liposomes by addition of ABA vesicles (25  $\mu$ M lipids and 28  $\mu$ M ABA). Liposomes were labeled with NBD-PE and Rhod-PE. Prior to ABA addition, FRET causes an extinction of NBD fluorescence ( $IF(t=0) < IF0$ ). After addition of ABA,  $IF(t)$  increases due to diminution of the FRET efficiency.  $IF0$  is the fluorescence after addition of 0.5% TX-100 corresponding to the absence of FRET. (B) Release of calcein revealed by a diminution of self-quenching. Prior to ABA addition calcein is concentrated in liposomes; release of calcein increased the fluorescence.  $IF0$  is the fluorescence after addition of 0.5% TX-100 corresponding to the complete release.

membranes. If domains had been formed, self-quenching, i.e., the slope of the curve, would be higher due to a higher local concentration of labeled lipids. The self-quenching was even lower than for the liposome at the same concentration ratio. This may originate from the higher size of ABA compare to lipids, which decreases the surface density of the probe at the same concentration. Thus, we conclude that lipids disperse homogeneously among the ABA molecules of the nanoparticle membrane for concentration ratios below 20 mol % of lipid.

For higher lipid to ABA ratios, differential scanning calorimetry (DSC) was more appropriate to investigate lipid distribution. We analyzed the effect of ABA addition into the chloroformic DPPC solution, during the preparation of liposomes via the film hydration technique. The insertion of the copolymer into the liposomal membranes has been extended by freeze–thaws cycles.<sup>27</sup> As shown in Figure 6, the endotherm for pure DPPC liposomes features a small tilted to rippled phase transition (at a pretransition temperature  $T_p$ ) and a main gel to liquid-crystalline phase transition at a melting temperature ( $T_m$ ) of  $41.5 \pm 0.05$  °C. ABA alone did not exhibit any phase transition above 0 °C, as expected for large polymers. In mixed vesicles, the pretransition peak observed with lipids disappeared upon increasing the ABA concentration. As already reported, this peak is sensitive to small amounts of contaminants.<sup>28</sup> Following addition of ABA in lipid vesicles, the main transition peak diminished and a second one appeared on its low-temperature side. Upon increase of the concentration to 40 mol %, this peak became more and more distinct from the actual main transition peak of DPPC. Whereas the temperatures of both the secondary and the main transition peak remained unaffected by the increase of polymer concentration, their intensities diminished. According to Baekmark et al.,<sup>29</sup> the appearance of the secondary peak should not be interpreted as a segregation phenomenon but rather as two conformational states of ABA in lipid membranes. In the low concentration

regime, the hydrophilic side blocks of the polymer are widely separated and only the hydrophobic B-block effectively interacts with the lipid membrane, thus reducing the enthalpy of the main transition. When the copolymer concentration is increased, the external A-blocks start to congest each other, and van der Waals repulsive forces between the side blocks start to considerably contribute to the membrane integrity and modify lipid packing.<sup>30</sup> Upon further increase of the ABA concentration, lipids become so widely separated from each other that the minimum cooperative unit can no longer be formed, and hence the obtained scan resembles that of ABA alone. Hence, as observed for fluorescence quenching, it can be concluded that ABA homogeneously distributes in liposomal membranes.

**Encapsulation Efficiency of Mixed Nanovesicles.** In the film hydration method, encapsulation of protein into liposomes occurs during freeze–thaw cycles, which rupture the lipid membrane, allowing the equilibration of protein concentration between the intraliposomal compartment and the surrounding medium.<sup>20</sup> With lipid, the encapsulation efficiency was equal to 3.5%, corresponding to the ratio of internal to the total volume. With ABA, the encapsulation efficiency is negligible and freeze–thaws do not help the entrance of protein inside the capsules (Figure 7). Upon addition of ABA in the lipid film, the encapsulation efficiency diminished with a transition between 20 and 30% ABA to lipid. This suggests that encapsulation of protein in liposomes was affected by the presence of ABA due to the formation of mixed structures.

**Exchanges between ABA Particles and Liposomes.** FRET may be used to monitor lipid dilution occurring during material exchange between two particles.<sup>24</sup> Fluorescently labeled liposomes containing NBD-PE and Rhod-PE were mixed with ABA polymersomes obtained by the ethanol injection method. Excitation of NBD at 490 nm results in an emission at 530 nm, which is reduced by the resonance energy transfer to rhodamine when the two lipids are in close proximity to each other. If molecule exchange occurs between liposomes and polymersomes, it would increase the distance between NBD and Rhod, thus leading to

(27) Castile, J. D.; Taylor, K. M.; Buckton, G. *Int. J. Pharm.* **1999**, *182*, 101–10.

(28) Biltonen, R. L.; Lichtenberg, D. *Chem. Phys. Lipids* **1993**, *64*, 129–42.

(29) Baekmark, T. R.; Pedersen, S.; Jorgensen, K.; Mouritsen, O. G. *Biophys. J.* **1997**, *73*, 1479–91.

(30) Hristova, K.; Kenworthy, A. K.; McIntosh, T. J. *Macromolecules* **1995**, *28*, 7963–99.

an increase in fluorescence at 530 nm, i.e., a decrease of FRET. As shown in Figure 8, incubation of ABA particles with liposomes results in an increased fluorescence originating from a reduced FRET efficiency. Interestingly, we found that the fluorescence depends on the liposomal composition and pH. PE-rich liposomes were more sensitive to ABA incubation than liposomes rich in PC or PS. The characteristic cone structure of PE which creates hydrophobic defaults on the membrane<sup>31</sup> may facilitate insertion of ABA. Fluorescence did not stabilize, even after 6 h of recording, featuring a slow equilibration to hybrid particles. In addition, lipid dilution is a function of pH. The charge of the polar head might change the lipid packing, shape, and phase transition temperature, thus facilitating or inhibiting ABA insertion into the membrane.<sup>32</sup>

This observation evokes the question about the orientation of monomer exchange: do lipids insert into polymersomes? Or do ABA monomers insert into liposomes? To tentatively answer this question, we loaded liposome with calcein and recorded its release upon ABA addition. We observed a transient calcein efflux (Figure 8B) as observed for insertion of peptides in lipid bilayer.<sup>33</sup> This suggests that ABA inserted into liposome membranes. This is consistent with the difference in the critical aggregation concentration (cac) of ABA (16  $\mu\text{M}$ )<sup>12</sup> and the critical micellar concentration (cmc) of lipids (below 1 nM).

(31) Chernomordik, L. *Chem. Phys. Lipids* **1996**, *81*, 203–13.

ABA vesicles are more stable than liposomes since they are resistant to dehydration and to freeze thaw fractures. Mixing ABA and lipids led to a hybrid membrane with intermediary properties, i.e., stability against dehydration but reduced loading capacities by freeze–thaw. As post-addition of ABA to liposomes may result in mixed vesicles as pluronic F-68 stabilizes membranes,<sup>34,35</sup> the encapsulation efficiency of liposomes could be used to load the capsules, which, afterwards, will be stabilized by insertion of ABA molecules.

**Acknowledgment.** We are most grateful to Alexandra Graff for her guiding advice, and Lisa Salleron, Luminita Damian, and Laurent Roux for technical support. We thank Lipoid for the gift of egg-PC. This research was supported through the EU-RTN network Nanocapsules with functionalized surfaces and walls (HPRN-CT-2000-00159), ACI nanosciences (NN/02 2 0147), and the CNRS project on “Protéomique et génie des Protéines”. Financial support by the NCCR Nanoscale Science is acknowledged.

JA043600X

(32) Tocanne, J. F.; Teissie, J. *Biochim. Biophys. Acta* **1990**, *1031*, 111–42.

(33) Bonnafous, P.; Stegmann, T. *J. Biol. Chem.* **2000**, *275*, 6160–6.

(34) Palomares, L. A.; Gonzalez, M.; Ramirez, O. T. *Enzyme Microb. Technol.* **2000**, *26*, 324–331.

(35) Firestone, M. A.; Wolf, A. C.; Seifert, S. *Biomacromolecules* **2003**, *4*, 1539–49.